

Electron Beam Lithography and It's application in Nanoscale Fabrication

Ashutosh Acharya, Sourav Sahoo

Gandhi Institute of Excellent Technocrats, Bhubaneswar, India

Modern Engineering & Management Studies, Balasore, Odisha, India

ABSTRACT—Miniaturization is the central theme in modern fabrication technology. Many of the components used in modern products are getting smaller and smaller. In this paper, the recent development of the electron beam lithography technique is reviewed with an emphasis on fabricating devices at the nanometer scale. Because of its very short wavelength and reasonable energy density characteristics, e-beam lithography has the ability to fabricate patterns having nanometer feature sizes. As a result, many nanoscale devices have been successfully fabricated by this technique. Following an introduction of this technique, recent developments in processing, tooling, resist, and pattern controlling are separately examined and discussed. Examples of nanodevices made by several different e-beam lithographic schemes are given, to illustrate the versatility and advancement of the e-beam lithography technique. Finally, future trends in this technique are discussed.

Index Terms—Direct writing, e

beam resist, electron beam lithography, nanodevices, nanofabrication, nanotechnology, projection printing.

I. INTRODUCTION

MINIATURIZATION and performance improvements are driving the electronics industry to shrink the feature size of semiconductor devices. Because of its diffraction limit, conventional optical or ultraviolet photolithography is becoming increasingly inadequate. As an example, even the refractive optical lithography is anticipated to reach its limit at a wavelength of 157 nm, beyond which significant issues arise in terms of availability of light sources, masks, and the need for new photoresist materials (SIA, [22]). Other lithography techniques, which use different forms of radiation, including extreme UV, x-ray, electron beams, and ion beams, to offer higher resolution, are growing in importance. A great deal of research has been done on these techniques to scale lithography technology down to the nano-scale arena (Brodie and Muray, [3], Timp, [9]). In this paper, the electron-beam lithography (EBL) technology will be reviewed. The latest developments, including the beam sources, system, process, resist, and application, are examined and discussed.

Lithography is the process of transferring patterns from one medium to another. For many years, particle beams of various types have been used in lithography. The electron source has the benefit of extremely high diffraction-limited resolution and has been used for transferring patterns having nanometer feature sizes. Recently they have become the popular selection in making nanoscale structures, by both direct writing and projection printing techniques. In the semiconductor industry, EBL has been routinely

used to generate master masks and reticles from computer-aided design (CAD) files [7]. These masks are usually used in optical projection printing to replicate the patterns on silicon wafers. EBL has begun to find applications in indirect writing, where the focused beam directly impinges on the resist in order to perform various activities. The definition of nanoscale lithography here follows that provided by the US National Science Foundation, and it can be interpreted as using lithographic tools for fabrication of any structures having feature sizes less than 100 nm. Nanoscale lithography is a large collection of nanofabrication techniques that have originated from the semiconductor industry. It normally removes or adds material on a substrate, similar to adding bricks or digging holes to construct a building. The planar processes in the IC industry are inherently batch-fabrication techniques that enable parallel production of a large number of highly precise electronic circuits through a single pass of processing sequences. Nanoscale lithography benefits from the same precise batch-fabrication processes in the creation of nanoscale devices. In this paper, the technologies of projection printing and indirect writing are reviewed. The other types of lithography, including proximity printing and contact printing, are not included in this paper because they have very limited flexibility and no rigorous effort have

been reported to specifically improve the current systems. In the following section, the present status of both the projection printing and direct writing systems is first assessed. The e-beam resists developed for different applications are then examined; the newly developed resists and the error sources in patterning and dimension control are also discussed. To illustrate several newly developed direct writing lithography techniques, the nanostructures recently fabricated by these techniques and their applications are represented in some detail. Finally, concluding remarks on future trends of the

beam lithographic technologies are given.

II. PROCESS AND SYSTEM

The main advantages of e-beam lithography over the conventional photolithography techniques include very high resolution and versatile pattern formation. In general, two distinct

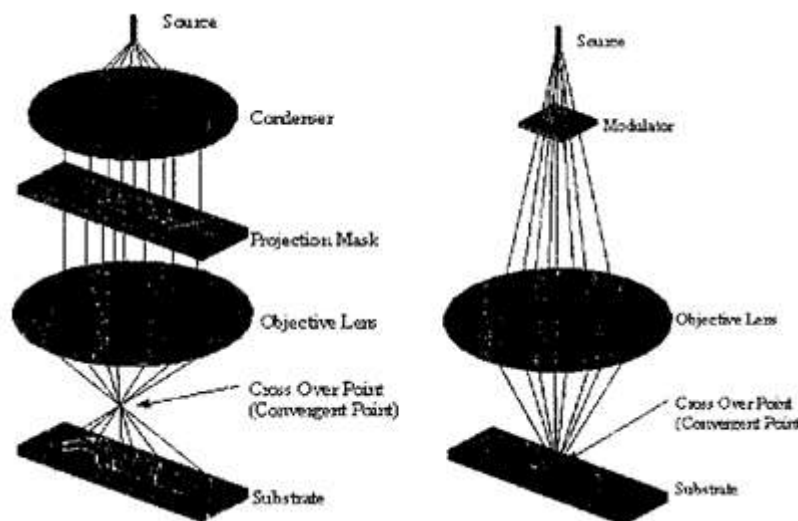


Fig. 1. Schematic of direct writing and projection printing.

schemes, projection printing and direct writing, are used in EBL. As shown in Fig. 1, in projection printing, a relatively large-sized electron-beam pattern is projected in parallel through the mask onto a resist-coated substrate by using a high-precision lens system; in indirect writing, a small spot of the electron beam is written directly onto a resist-coated substrate, eliminating the expensive and time-consuming production of masks. Recent developments in these two schemes are represented in this section.

A. Projection Printing

Several versions of projection EBL systems have been developed. Bell Laboratories started the projection EBL development with the invention of the Scattering with angular limitation in projection electron-beam lithography (SCALPEL) system in 1989 [2], while IBM had laid the foundation for its projection reduction exposure with variable axis immersion lenses (PREVAIL) technology with the development of the variable-axis lens for electron-beam lithography systems during the 1980s [17], [18].

Both concepts project a small field image of a mask onto a wafer to generate nanoscale subpatterns.

The short penetration length of electrons, however, precludes the use of a solid substrate, like quartz, for the mask. A very thin membrane mask can be used; otherwise, a stencil mask with cutouts through which beams can pass is needed. These mask difficulties and other problems, including stitching a great number of subpatterns into a single overall pattern, the aberration limitation, and excessive thermal absorption or expansion, are sufficient to prevent the projection EBL from being a completely practical tool for nanofabrication.

The strength of SCALPEL, which differentiates it from previous attempts at projection EBL, lies in its specially designed mask, also known as the scattering mask. The SCALPEL mask consists of a low-atomic number membrane, on which a layer of the pattern made of a high-atomic number material is coated. When the electrons pass through the high-atomic number material, they scatter more strongly and at higher angles than those that pass through the low-atomic number

membrane. As illustrated in Fig. 2, an aperture located at the back focal plane of the projection lens blocks the strongly scattered electrons, while those passing through the membrane suffer little

change to their trajectories and travel through the aperture. As a result, the unblocked electrons that pass through the aperture form a high

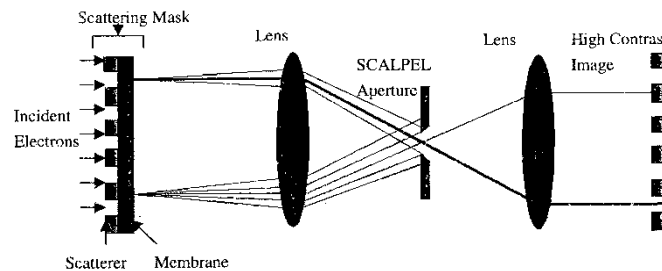


Fig. 2. SCALPEL principle of operation.

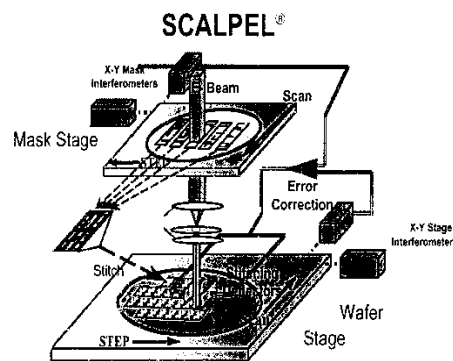


Fig. 3. Schematic of SCALPEL proof-of-concept system (with permission by Lucent Technologies).

contrast image printed on the wafer or substrate plane. The typical SCALPEL mask is a thin nitride film (about 100 nm thick) on top of which a tungsten pattern (50 nm thick) is placed. Since the incident electron energy is not only absorbed by the mask but also blocked by the aperture, thermal distortion of the mask can be minimized.

To avoid the excessive distortion by field aberrations of electron optics, the field size of an electron beam that can be projected through a mask on the wafer is kept relatively small, in the order of 1-mm. The small field size or printing area has presented a major concern to the SCALPEL system. In order to image a full 300-mm wafer, the entire wafer has to be exposed sequentially by stitching these small fields together with high accuracy. Strict mechanical positioning of mask and wafer to accomplish field stitching would be limited by stage acceleration and speed, and would result in prohibitively low throughput. Fig. 3 shows a SCALPEL proof-of-concept system developed by Lucent Technologies [12] using the step-and-scan

writing strategy instead of the step-and-repeats scheme normally used in photolithography system. As shown, x-y mask interferometers on top help in the positioning of the beam. Below it is the mask stage with the pattern. It also shows the focusing lenses and the wafer stage where the stitching operation is shown. An error correction module is included in the schematic. Also the direction of the step and scan is shown in the diagram.

In the PREVAIL approach, the small fields in both reticle and wafer are stitched through a combination of high-speed electronic beam scanning and moderate-speed mechanical scanning. The cornerstone of the PREVAIL approach is a system of variable-axis lenses. The variable-axis lens permits shifting of the electron optical axis along a predetermined curvature, while simultaneously deflecting the electron beam to precisely follow the curvilinear variable axis so that the

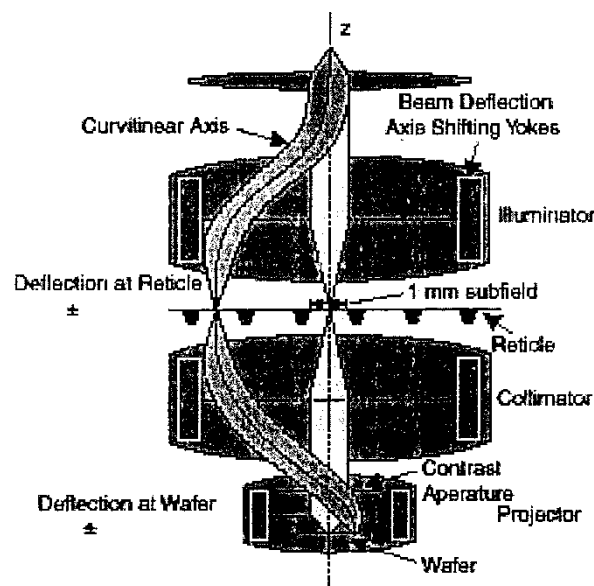


Fig.4.PREVAIL imaging concept concept [18].

beam effectively remains on the axis, eliminating all off-axis aberrations. This task is performed through the superposition of various magnetic deflection fields. Fig. 4 shows the basic PREVAIL imaging concept [18]. The illuminator is a magnetic lens that system provides illumination for each field pattern by imaging a 11-mm shaped beam onto the reticle. Collimator and projector lenses form an antisymmetric telecentric doublet known to inherently possess minimal geometric aberrations. The curved beam paths schematically illustrate the illumination and imaging of a field at the edge of the optical field of view. A proof-of-concept PREVAIL system has recently achieved an enhanced field size or printing area of 10 mm [6]. This result makes the PREVAIL approach promising, but further improvement is needed because larger scan ranges are required for the illumination and projection of the reticle, and also because the enhanced pattern field (10-mm) is still orders of magnitude smaller compared to the size of the current 300-mm semiconductor wafer. Other projection EBL attempts, including the multiple column (or beam) system developed by ETEC, an Applied Materials-owned company, are in much earlier stages as compared with the status of SCALPEL and PREVAIL. The challenge for all of these emerging technologies is to downscale the feature size while maintaining a high throughput. To increase the throughput and the quality of the product, the advantages of techniques used in SCALPEL, PREVAIL, and multi-column systems will eventually be integrated into one system. Once integrated, the projection EBL can become in the next generation

lithography mainstream in the semiconductor industry.

B. Direct Writing

Direct writing is the most common EBL approach. Derived from the early scanning electron microscopes, the direct writing EBL has been used for a variety of applications since the late 1960s and many commercial systems have been developed since then. Normally, the direct write systems use a finely focused Gaussian round beam that moves with the wafer to expose the wafer one pixel at a time, and can be classified as raster scan or vector scans, with either fixed or variable beam geometry. Basically, as shown in Fig. 1, a direct writing system consists of a source of electrons, a focusing optics set, a blank to turn the beam on and off, a deflection system for moving the beam, and a stage for holding the substrate.

The direct writing EBL can be used for generating extremely fine patterns; in fact, when combined with etching and deposition processes, fabrication of future electronic devices with critical dimension as small as 10 nm has been demonstrated [11]. Since direct writing EBL is capable of superior resolution and requires no expensive projection optics or time-consuming mask production, it is the most desirable process for cutting-edge micro and nanofabrication. However, direct writing transfers the pattern by exposing one pixel or one image element at a time. This imposes a limitation on the exposure speed or the rate of the pattern to be transferred onto the wafer. This throughput handicap has confined the direct writing system to a supporting role in the semiconductor industry; it has applications in niches: mask making, prototyping, fabric

ation of small volume special products, and research and development for advanced applications [13]. Recently, considerable effort has been dedicated to the variable shaped beam technology to increase its throughput by enhancing exposure speed and to widen its applications by integrating with other nanoscale processes. The shaped beam system uses parallel electron beam to write a primitive shape (mainly rectangles) in one shot. These primitive shapes are smaller than the field sizes achieved in the projection EBL systems mentioned earlier. In the shaped beam system, the upper aperture in the optics is typically used to form two sides of a rectangle, and the overlay of the lower aperture constructs the other two sides. More complex shapes can be achieved by splitting the rectangle before the exposure. The shaped beam system gains the speed or throughput by compromising the resolution achieved by the single pixel of the Gaussian beam system. In spite of sizable enhancements, the throughput of shaped beam systems in terms of wafers per hour has actually declined; this is due to the continually increasing density and complexity of ICs and expanding wafer size [17]. Since the shaped beam tool is more

complicated than the fixed spot (Gaussian beam) system, the trade-off between pattern generation flexibility and resolution with pattern writing speed will be a major concern for future development of the shaped beam technology. It is believed that Gaussian beam direct writing will still play a major role in nanofabrication because of the continuing shrinkage of devices and its combined superiority in flexibility, resolution, precision, and cost.

C. Lift-Off Process and Others

The most popular process used in direct writing EBL is the lift-off process; it is an additive process that adds material to the substrate. The lift-off process consists of several steps: e-beam resist coating, exposure, and development. The normal lift-off process is schematically explained in Fig. 5. The top figure [Fig. 5(a)] shows that the resist coating is exposed by e-beam direct writing using a vector or raster scan, while Fig. 5(b) shows that the exposed resist (the nanostructure pattern) is developed

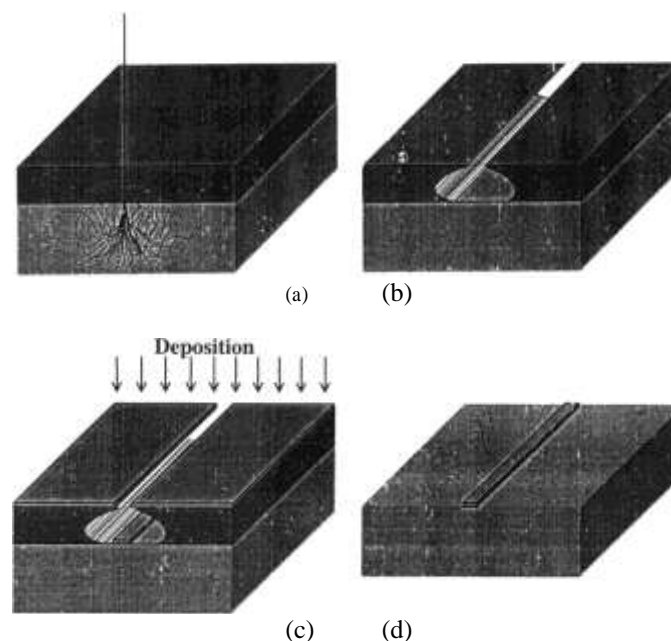


Fig. 5. Schematic of EBL lift-off process: (a) electron beam injection with scattering, (b) exposed resist developed and removed, (c) deposition of desired materials by e-gun or vacuum evaporation, and (d) lift-off of unwanted materials.

and removed in a solvent. A metal layer (the nanostructure material) can be deposited by an e-gun or an evaporation process on the substrate, as depicted in Fig. 5(c). The final step of the lift-off process is accomplished by soaking the substrate in a solvent bath (e.g., acetone for PMMA resist) to wash

away the remaining resist and unwanted material. The final deposited nanostructure on the substrate is shown in Fig. 5(d). Frequently, the lift-off process prefers a thick resist layer for forming undercut profiles and good adhesion with the substrate for the subsequent additive or subtractive

processes. Since these etching or deposition processes are very similar to those in the conventional photolithography process, their procedures and requirements can be found in most semiconductor processing textbooks and are not repeated here.

III. E-BEAM RESISTS

Electron beam resists are normally coated onto the substrate to record the image of the pattern to be transferred. The final pattern made by the EBL is a relief structure in the coated resist layer representing the pattern being exposed. In this section, a few standard resist systems will be presented.

Some useful recipes can be found in sections where the fabrications of specific nanostructures are presented. In depth reviews of this subject can be found in Reichmanis and Novembre [19] and Helbert and Daou [8].

Usually, the e-beam resists are high molecular-weight polymers dissolved in a liquid solvent. The polymer changes its structure when exposed to radiation, including electron radiation. Electron beam resists can be either positive or negative. After exposure to electrons, the positive resists are weakened by the scission of main- and side-chains and the exposed resists become more soluble in the developing solution. A solvent developer selectively washes away the weakened or lower molecular-weight resist; thus, a positive tone pattern is formed in the resist film. On the other hand, the negative resists are strengthened during exposure by a radiation-initiated cross-linking reaction and become less soluble in the developer. After the resists are developed, the pattern is transferred to the substrate through the lift-off process mentioned earlier.

A. Positive Resists

Polymethyl methacrylate (PMMA) was one of the first resists developed for EBL and remains the most commonly used positive resist that has a moderate glass transition temperature of

114°C. The PMMA comes in powder form and is dissolved in a solvent, such as anisole or chlorobenzene, of desired concentration. The resist liquid is dropped onto the substrate and then spun at high speed to form a thin coating. This is followed by soft bake processing at temperatures ranging from 130°C to 170°C with a hot plate or oven to bake out the casting solvent. The final resist thickness is determined by the PMMA concentration and by the spin speed. For instance, 950 K PMMA (2% in anisole) resist spun at 3000 rpm would result in a

thickness of about 200 nm. The dose values of the electron beam used for exposure range from 100 to 500 C/cm [Fig. 5(a)]. The typical developers used are 1:3 methyl isobutyl ketone: isopropanol (MIBK:IPA) for the highest contrast and 1:1 MIBK:IPA for the highest sensitivity [1]. The developed region is then removed by rinsing in pure IPA for 30 s.

PMMA has extremely high resolution, and its ultimate resolution has been demonstrated to be less than 10 nm [11]; its major problems are its relatively poor sensitivity, poor dry etch resistance, and moderate thermal stability. The copolymer, Methyl Methacrylate and Methacrylic Acid [P(MMA-MAA)], provides a three- to four-fold improvement in sensitivity relative to PMMA and image thermal stability of 160°C. Since P(MMA-MAA) can also be developed in MIBK:IPA solvent as used for PMMA, a single-step development of mixed layers of PMMA and P(MMA-MAA) is possible for enhancing the sensitivity and thermal stability of the resist. Other

important positive resists include PBS (Polybutene-1-Sulfone) and EBR-9 (a copolymer of trifluoroethylchloroacrylate and tetrafluoropropyl α -chloroacrylate) which have high sensitivity and ZEP (a copolymer of chloromethacrylate and methylstyrene) which has high resolution. It is noted that the desired properties of a resist are high resolution and high sensitivity (high speed). Unfortunately, the resist that have higher sensitivity, including those mentioned here, usually have lower resolution, especially compared to PMMA.

B. Negative Resists

Negative resists tend to have less bias but they have problems with scum and swelling during development

and bridging between features. Popular negative e-beam resists consist of the Shipley advanced lithography (SAL) product line, an epoxy copolymer of glycidyl methacrylate and ethylacrylate [P(GMA-EA)], also known as COP, and a partially chloromethylated polystyrene (CMS). Also, PMMA can exhibit negative tone when exposed to a dose one order of magnitude higher. While COP has high sensitivity, CMS possesses modest resolution at modest sensitivity.

The SAL offers many new deep-ultraviolet (DUV) resists through the use of chemically amplified (CAP) resist materials. Fast versions of CAP, such as SAL 601-ER7 (a negative resist) have demonstrated high-resolution capability with 100 nm lines at a sensitivity higher than PMMA. The use of DUV resists in EBL also opens up the possibility of exposing the resist layer to both DUV steppers and EBL machines before development, so that large areas can be exposed

ith medium-to-low-resolution by the fast DUV stepper, whereas the high resolution details can be exposed by the accurate but slow EBL. This approach, also known as mix and match technology, can achieve the high-resolution detail in critical areas but requires less exposure time.

IV. PATTERN VARIATION

The electron de Broglie wavelength of a typical EBL operating condition, 50 keV, is less than 10 pm or 0.01 nm, which is far below typical atomic sizes. Hence, diffraction is not a limiting factor of the resolution. Ideally, e-beam diameters are possible on the order of 1 nm. However, beam-material or scattering interaction degrades this limit significantly [16].

A. Scattering or Proximity Effect

When the electron beam strikes the resist solid, many of the electrons experience small-angle forward scattering, which tends to enlarge the initial beam size. As the electrons penetrate through the resist into the substrate, some of them undergo large-angle scattering events leading to backscattering, in which these electrons return back through the resist in a region far from the desired exposure. This causes additional exposure in the resist and is also known as the e-beam proximity effect. Also, as the primary electrons slow down, much of

the energy is dissipated in the form of secondary electrons in which a small portion may have significant energies, on the order of 1 keV. These so-called fast electrons are responsible for the bulk of actual resist exposure and can contribute to the proximity effect in the range of a few tenths of a micron [13].

B. Remedy

The net results of scattering electrons cause the dose delivered by the e-beam not to confine to the original shape, resulting in pattern variations. Thus, many different approaches have been developed to alleviate the proximity effect or minimize pattern variation. Some simpler remedies include using a thin resist that is less than the feature size or a thin coating between the resist and the substrate to partially "filter" the secondary and some backscattered electrons.

The most systematic way is dose control. Different feature sizes have different dose requirements. If the pattern is uniform, the overall dose is simply adjusted until the desirable pattern size is achieved. If the pattern is rather complex, dose modulation should be considered. The specific dose assignments are often made at fracture time by filtering shape according to size, and can be placed on separate data files in the CAD tool used in EBL. Commercial CAD tools, such as SELID and CAPROX by SIGMA-C, and PROLITH by KLA-Tencor, have become available for simulating e-beam exposure, as well as for correcting the proximity effect [5], [15].

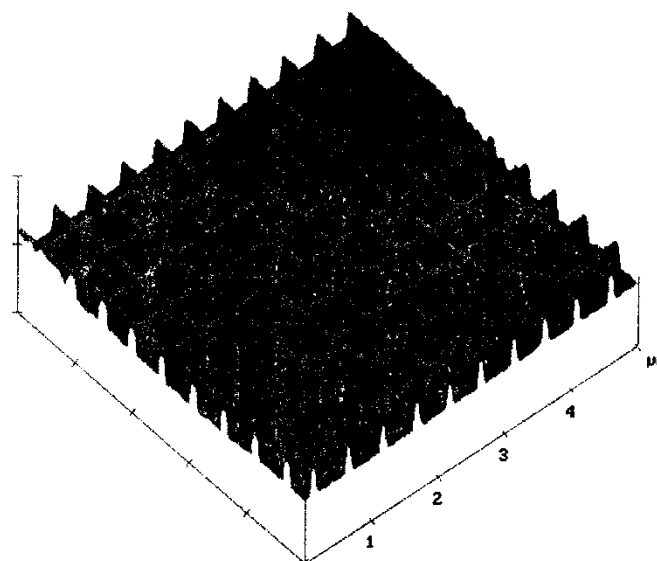


Fig. 6. AFM Image of EBL fabricated Au-Mesh.

Other error sources for pattern variations include the path-buttering error, resolution of the resist, nonuniform resist

temperature, beam current instability, spot size instability, and beam deflection error [10].

V. FABRICATION

The fabrication processes for making four nanostructures are presented in this section to illustrate the standard and nonstandard lift-off techniques as well as the applications involved.

A. Nano-Mesh Pattern

A gold mesh pattern on a silicon substrate used for calibration of atomic force microscope is first presented to illustrate an nanostructure made by the standard lift-off process described in Fig. 5. The mesh pattern is designed in a CAD program and is loaded into the control system of an electron beam writer, normally controlled by software loaded on a PC.

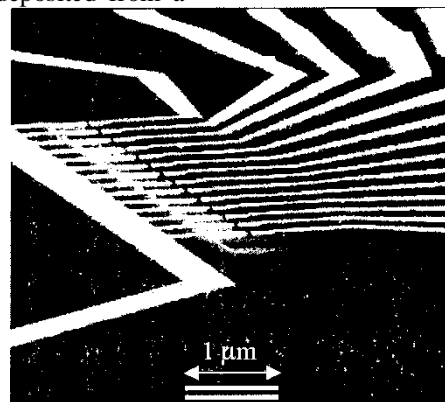
The Si substrate is coated with a 200-nm thick PMMA resist and an area dose of 250C/cm is used for exposure. The exposed region is then developed and removed. After developing, the sample is also subjected to an oxygen plasma cleaning process (85 mTorr, 40 W, 45 s) to ensure a residue-free image. Gold is then deposited from a

small source onto the substrate and resist by thermal evaporation [Fig. 5(c)]. An AFM image of the fabricated mesh pattern is shown in Fig. 6. Both the width and height of the mesh line are 40 nm, while the mesh line spacing is approximately 500 nm.

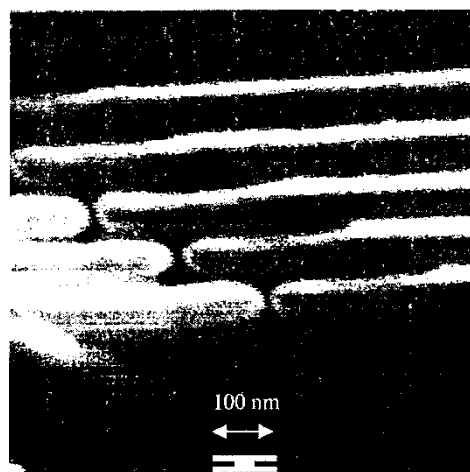
It is noteworthy that because of the backscattering of electrons mentioned earlier, the lower part of the resist receives more dosage than its surface, resulting in a slightly undercut profile along the edges of the pattern [see Fig. 5(b)]. This undercut provides a clean separation of the deposited material and, hence, a sharp lift-off pattern.

B. NanoBimetal-Electrodes

The lift-off process can be combined with other nano-processes to make complex devices. Manufacturing of a nanoray



(a)



(b)

Fig.7. Nano-electrode Pairs (a) SEM image of Cr electrodes fabricated on SiN/SiO/Si-substrate and (b) enlargement of electrode structures.

of nano-scale electrode pairs is presented in this subsection. Fig. 7(a) shows a scanning electron microscope (SEM) picture of the resulting nano-structure; the two oppositely pointed Au-electrodes [Fig. 7(b)], acting as source and drain, consist of a 10 nm-thick Cr bottom layer, which is used as an adhesion layer, and a 25 nm-thick Au top layer. The width of the electrodes is about 160 nm, and the spacing between them is 400 nm. The gap between the electrodes is about 15 nm. The two Au electrodes are made relatively wider so as to sustain themselves without a substrate.

The substrate is a standard Si wafer covered by a 100 nm-thick LPCVD-grown Si₃N₄ and a 300 nm-thick thermally grown SiO₂ layer. A window on the Si₃N₄/SiO₂ layer beneath the gap is defined by the lift-

off process and accomplished by CF/O plasma reactive ion etching of Si₃N₄ layer and HF wet etching of SiO₂ layer. The underlying Si₃N₄/SiO₂ are etched out to form a window so that the applied electric field between electrodes can be highly concentrated. Nanoparticle can be allocated in the gap between the electrodes as a self-assembly process, which follows this stage of fabrication [21].

C. Non-Conducting Substrate Using Bilayer Resist
 The EBL process using a bilayer resist for a bow-tie structure on an insulating substrate is presented. The lithography system

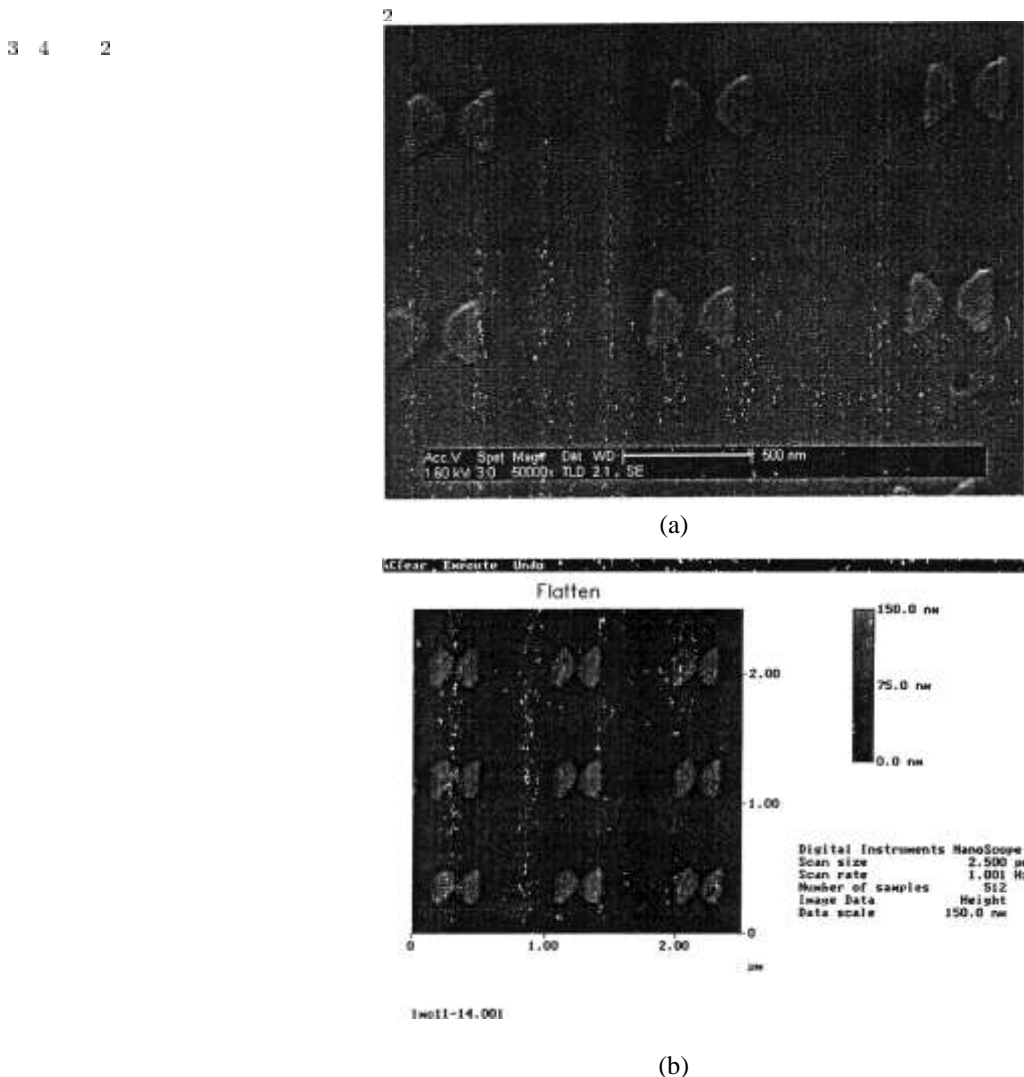
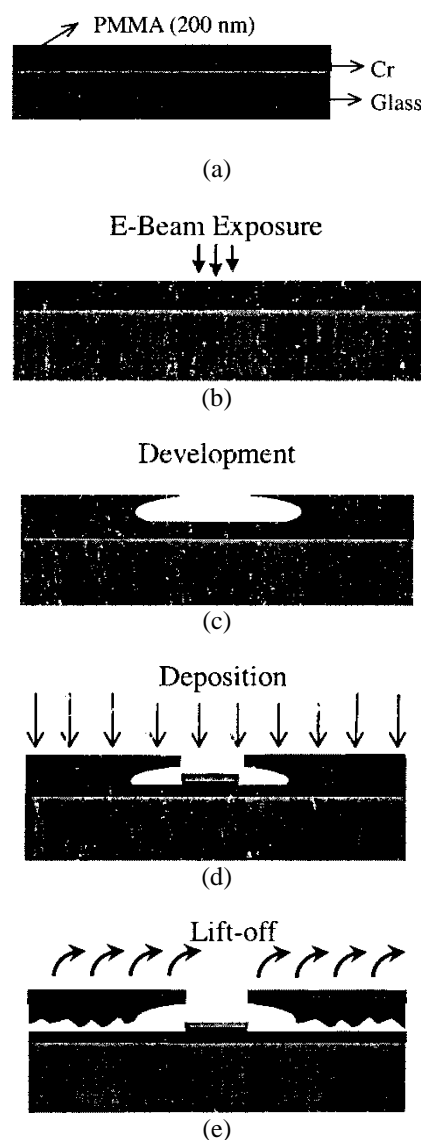


Fig. 8. Bilayer nano-bow-tie structures on a glass substrate using bilayer resist: (a) SEM image and (b) AFM image.

used is converted from Hitachi 54200 scanning electron microscope using a vector scan procedure. The bowtie structure is a major component of an next-generation optical probe. The optical probe is based on a concept, called the wave interrogated near-field array (WINFA), which combines the sensitivity of near-field detection with the speed of optical scanning [14]. It is expected that bowties having a 40-nm gap should act as resonant elements to provide spatial resolution well below the optical diffraction limit with high transmission efficiency approaching unity. The fabricated bowtie-structure is designed for the inci-

dent source having a wavelength in the neighborhood of 500-nm (green light) since the illuminated orgap area is approximately one eighth to one twelfth of the source wavelength. It is expected that voids or particles 50-nm in size or smaller can be identified. As a design requirement, the substrate of the bowties should be transparent to the incident wave source, and thus, a glass-based substrate is used. However, when patterning an insulating glass substrate, the substrate charging causes considerable distortion. To cope with the distortion problem, also known as the discharge accumulation [13], a bilayer resist is used in EBL. The bilayer resist consists of a conducting layer sandwiched by a polymer resist layer and the substrate, which is used to eliminate



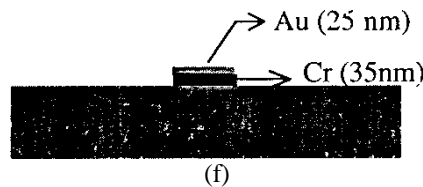


Fig.9. Lift-off process using bilayer resist: (a) deposit Cr and spin-coat PMMA, (b) patterning, (c) creating undercut in PMMA, (d) depositing 5-nm Cr and 25-nm Au, (e) removing unwanted materials, and (f) wet etching with Au mask to remove unprotected Cr.

the charge accumulation problem. Fig. 8(a) shows a SEM image of the bowtie array fabricated on a 0.5-mm-thick Pyrex glass substrate; the gap of the fabricated bowties can be observed to be approximately 40 nm.

To prepare the bilayer system, a 30-nm thick Cr film is first coated on the Pyrex glass substrate by thermal evaporating process. Then a PMMA resist film is spin coated to cover the Cr layer [Fig. 9(a)].

As the pattern is defined on this top layer, a thinner film is preferred, as it would produce a better pattern sharpness. A diluted PMMA resist (2% in anisole), spun at 3000 rpm, is used. After soft-baking at 135 °C, a thin (5 nm) PMMA resist film is formed. The bilayer resist is then exposed with an areal dose of approximately 250 C/cm² [Fig. 9(b)]. The

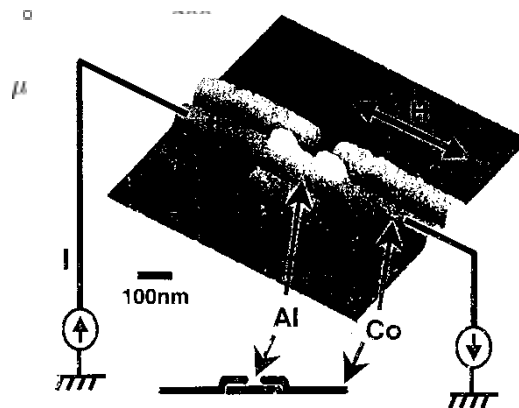


Fig.10. AFM image of FM/SC/FM transistor and biasing circuit.

exposed region is developed, removed, and cleaned to insure a residue-free image [Fig. 9(c)]. A 5-nm Cr is deposited first while a 25-nm Au is then deposited [Fig. 9(d)]. The unwanted materials are lifted off [Fig. 9(e)]. The Au layer then acts as a mask while the unprotected Cr is removed by the chrome wet etching process [Fig. 9(f)]. A relative thick structure can be formed by the bilayer resist technique because the structure consists of two layers. The corresponding AFM image of the bowties is shown in Fig. 8(b). The thickness of the bilayer bowtie can also be estimated from the image; it is around 60 nm; it has a 25-nm Au layer on top of a 35-nm thick Cr layer.

In addition to making a thick structure, the bilayer resist scheme is not only to cope with the charge accumulation problem caused by a nonconducting substrate but also to eliminate the “lift-off flag” defects in which thicker materials appear along the bowtie edges when the standard or the single-layer resist lift-off process is employed.

D. Tandem Pattern by Tri-Layer Resist

Spin imbalance can lead to suppression of superconductivity. A ferromagnet-superconductor-ferromagnet (FM/SC/FM) single-electron transistor has been developed to use spin imbalance to effectively suppress the gap superconductivity with the goal for better control of its superconductivity at low temperatures within low fields [4]. The FM/SC/FM double tunnel junctions are made of the corresponding Co/Al/Co layers. The superconducting gap suppression can be turned on and off by manipulating mutual orientations of magnetic moment of the two Co leads. The effects of the suppression increase with increasing source-drain. The single-electron transistor (SET) is a potential candidate for the next generation of electronic devices because of its great advantages in low power consumption and high packing density.

Fig.10 show an AFM image and its biasing circuit of the Co/Al/Co transistor, while Fig. 11 is the corresponding magnetic force microscope (MFM) image obtained using low magnetic stray field and high coercivity CoPt tips. The inset in Fig. 10 illustrates the cross section of the island and

junctions. As shown in Fig. 11, the Co and Al electrodes are reindicated by solid and dashed lines, respectively. As shown, these two electrodes are similar in shape and run parallel with each other at 50 nm apart. As a result, the two electrodes can be fabricated by one mask using a tri-layer resist.

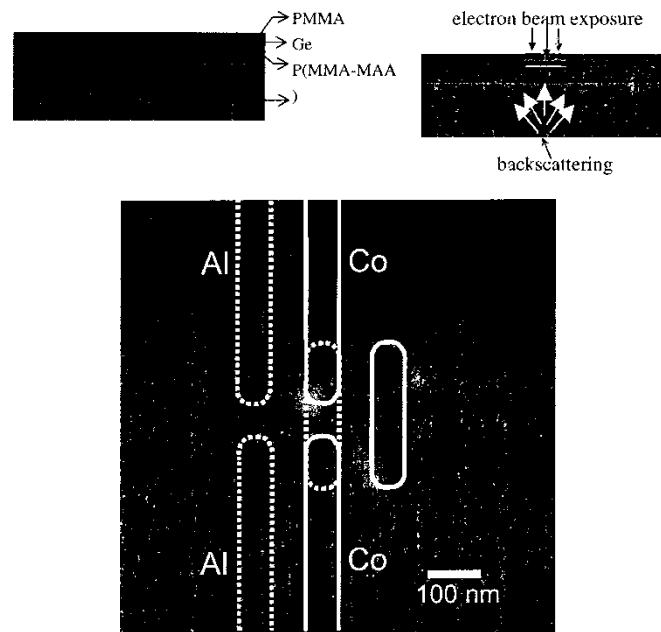


Fig. 11. MFM image of Co (solid line) and Al (dashed line) electrodes in FM/SC/FM transistor.

In preparation of a tri-layer resist, a thick bottom layer of the P(MMA-MAA) resist, acting as a spacer, is spun coated on the substrate and baked dry as shown in Fig. 12(a). With a coating spin speed of 4000 rpm and a baking temperature of 165°C, the obtained resist film is about 400 nm thick. This film is then covered with a 20 nm thick thermal-boat evaporated Ge layer. Ge is a good candidate not only for its conducting ability but also for its small granular size, allowing the generation of fine patterns. The top layer of PMMA resist film is then spin coated to cover the Ge layer. As the pattern is defined on this top layer, a thinner film is preferred, as it would produce better pattern sharpness. To this end, a diluted PMMA resist (2% in anisole), spun at 5000 rpm, is used. After soft-baking at 135°C, it forms a thin (100 nm) resist film. The trilayer resist is then exposed with an areadose of approximately 250 C/cm² [Fig. 12(b)], and the top PMMA resist is developed in solution for 1 minute, rinsed in IPA for 30 s [Fig. 12(c)]. The image is then transferred to the Ge layer underneath using a CF plasma etch process [Fig. 12(d)]. Since the pattern is defined by the thin resist layer of the high resolution PMMA on the top while the height and undercut are provided by the thick layer of high

sensitivity P(MMA-MAA) on the bottom, the resulting undercut of the pattern can be so large that it can allow narrow-separated tandem patterns (two parallel electrodes) to be formed. The germanium interlayer not only serves as a barrier to separate the top and the bottom polymer layers but also acts as an excellent mask for the subsequent deposition process. In patterning the bottom resist, as illustrated in Fig. 12(e), the substrate has to tilt slightly to allow for the creation of a larger and thicker undercut along the patterned edge. Using two evaporation incidences at different angles, the Co and Al electrodes can be separately patterned on the substrate as shown in Fig. 12(f); the distance between the two electrodes shown in Fig. 10 or Fig. 11 is approximately 50 nm. If the incidence angles can be controlled with high precision, the two electrode structures can be shifted to the desired location to form small overlap regions (the two hills in Fig. 10 and the inset), which act as the source and drain tunnel junctions. The transistor device presented here is similar to that produced by Chen, et al., [4]. As shown, the EBL process using a tri-layer resist is particularly convenient for

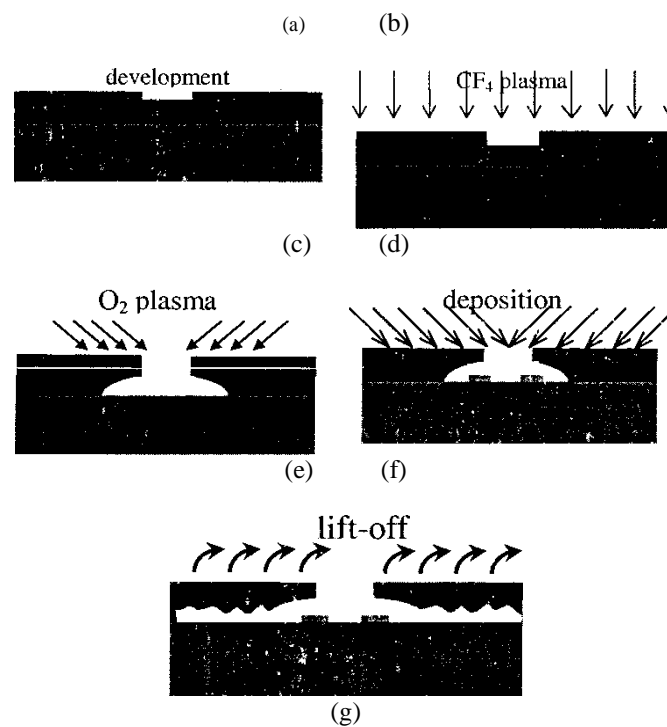


Fig. 12. Lift-off process using trilayer resist with two-angle evaporation: (a) trilayer resist on glass substrate, (b) resist exposed by electrons, (c) developed portion removed, (d) etched by CF_4 plasma, (e) oxygen plasma patterning with a tilted substrate, (f) two separated structures by two evaporations, and (g) lift-off of unwanted materials. fabricating two identical patterns where the gap of these two patterns can be extremely small, at the order of 10 nm.

VI. CONCLUSION

The current development of electron beam lithography in nanofabrication has been reviewed. Both the technologies of direct writing and projection printing are examined. A wide variety of equipment is available for performing the EBL. While the equipment for projection printing is still largely under development, the direct writing approach is a mature technology that ranges from a finely-focused Gaussian spot to a complex shape determined by different arrangements of apertures. Operating conditions also vary widely by changing the parameters, including beam energy, beam current, and beam deflection rate. Moreover, some machines write on stationary substrates, while others move the substrates. As a result, the patterns on the substrate or the fabricated nanostructures are significantly affected by these parameters and the design of the equipment.

The direct writing EBL has been the most flexible system in making a variety of nanodevices with critical dimensions below 10 nm. The direct writing approach will continue to play a major role in nanofabrication and be the de facto technique in maskmaking for other advanced lithographic processes. The versa-

tility of direct writing is also demonstrated on four different nanostructures created by the different EBL processes in this paper.

On the other hand, by considering the throughput, the projection printing EBL should have potential to be the most probable method among the next generation lithography (NGL) techniques for the semiconductor industry, although the prototype systems reviewed have indicated that further fine-tuning and improvement in their resolution and precision are needed. Particularly, the accuracy of the stitching scheme requires further refining, and resists with higher sensitivity and better

processing characteristics need to be developed. It is also critical that projection EBL should demonstrate the system level requirements to be included in the next generation lithography in the semiconductor industry.

The processes for fabrication of four nanostructures are specifically presented for illustrating the versatility of direct writing EBL. The illustrated applications of these nanostructures include calibration, electronics devices and optics components. A wide variety of other applications, from materials to energy and from cosmetics to health care, all look promising [20]. Nanofabrication will be a key technology

in the 21st century and will have a revolutionary impact on every aspect of the manufacturing industry. Tremendous challenges and opportunities await for us to explore.

REFERENCES

- [1] G. H. Bernstein, D. A. Hill, and W. Liu, "New high-contrast developers for poly(methyl methacrylate) resist," *J. Appl. Phys.*, vol. 71, no. 8, pp.4066–4075, 1992.
- [2] S. D. Berger and J. M. Gibson, "New approach to projection electron lithography with demonstrated 0.1 micron linewidth," *Appl. Phys. Lett.*, vol. 57, pp. 153–155, 1990.
- [3] I. Brodie and J. J. Murray, *The Physics of Micro/Nano-Fabrication*. New York: Plenum, 1992.
- [4] C. D. Chen, W. Kuo, D. S. Chung, J. H. Shyu, and C. S. Wu, "Evidence for suppression of superconductivity by spin imbalance in Co-Al-Co single electron transistors," *Phys. Rev. Lett.*, vol. 88, no. 4, pp.47001–47004, 2002.
- [5] Z. Cui, A. Gerardino, M. Gentili, E. Di Fabrizio, and P. Prewett, "Comparative study of AZPN114 and SAL601 chemically amplified resists for electron beam nanolithography," *J. Vac. Sci. Technol. B*, vol. 16, no. 6, pp. 3284–3288, 1998.
- [6] R. S. Dhaliwal, W. A. Enichen, S. D. Golladay, R. A. Kendall, J. E. Lieberman, H. C. Pfeiffer, D. J. Pinckney, C. F. Robinson, J. D. Rockrohr, W. Stickle, and E. V. Tressler, "PREVAIL: Electron projection technology approach for next-generation lithography," *IBM J. Res. Develop.*, vol. 45, no. 5, pp. 615–638, 2000.
- [7] S. K. Ghandhi, *VLSI Fabrication Principles: Silicon and Gallium Arsenide*, 2nd ed. New York: Wiley, 1994.
- [8] J. N. Helbert and T. Daou, *Handbook of VLSI Microlithography*, J. N. Helbert, Ed. Park Ridge, NJ: Noyes, 2001, ch. 2.
- [9] G. Timp, *Nanotechnology*. New York: Springer-Verlag/AIP, 1999.
- [10] J. Ingino, G. Owen, C. N. Berglund, R. Browning, and R. F. Pease, "Workpiece charging in electron beam lithography," *J. Vac. Sci. Technol. B*, vol. 12, no. 3, pp. 1367–1371, 1994.
- [11] M. Khoury and D. K. Ferry, "Effect of molecular weight on poly(methyl methacrylate) resolution," *J. Vac. Sci. Technol. B*, vol. 14, no. 1, pp. 75–79, 1996.
- [12] J. A. Liddle, L. R. Harriot, A. E. Novembre, and W. K. Wasikiewicz. (1999) SCALPEL: A projection electron-beam approach to sub-optical lithography. Tech. Rep., Bell Labs, Lucent Technol., Murray Hill, NJ. [Online]. Available: <http://www1.bell-labs.com/project/SCALPEL/9905.ngl/ngl199.pdf>
- [13] M. A. McCord and M. J. Rooks, *Handbook of Microlithography, Micro-machining, and Microfabrication*, P. Rai-Choudhury, Ed. Bellingham, WA: SPIE Optical Engineering, 1997, ch. 2, pp. 139–249.
- [14] A. A. Tseng, C. D. Chen, C. S. Wu, R. E. Diaz, and M. Watts, "Electron-beam lithography of microbowtie structures for next generation optical probe," *J. Microlithograph., Microfab., Microsyst.*, vol. 1, no. 2, pp. 123–135, 2002.
- [15] M. Simecek, A. Rosenbusch, T. Ohta, and H. Jinbo, "A new approach of electron-beam proximity effect correction for high resolution applications," *Jpn. J. Appl. Phys.*, pt. 1, vol. 37, no. 12B, pp. 6774–6778, 1998.
- [16] M. C. Peckerar, F. K. Perkins, E. A. Dobisz, and O. J. Glembocki, *Handbook of Microlithography, Micromachining, and Microfabrication*, P. Rai-Choudhury, Ed. Bellingham, WA: SPIE Optical Engineering, 1997, vol. 1, ch. 8, pp. 681–763.
- [17] H. C. Pfeiffer, "Advanced electron-beam systems for manufacturing," in *Proc. Electron-Beam, X-Ray, Ion Beam Submicrom. Lithograph. Manufact. II*, vol. 1671, M. Peckerar, Ed., 1992, pp. 100–110.
- [18] —, "PREVAIL: IBM's electron-beam technology for next-generation lithography," *IBM MicroNews*, vol. 6, no. 3, pp. 41–44, 2000.
- [19] E. Reichmanis and A. E. Novembre, "Lithographic resist materials chemistry," *Annu. Rev. Mater. Sci.*, vol. 1, pp. 11–43, 1993.
- [20] M. C. Roco and W. S. Bainbridge, Eds., *Societal Implications of Nanoscience and Nanotechnology*. Hingham, MA: Kluwer Academic, 2001.
- [21] S. M. Shih, W. F. Su, Y. J. Lin, C. S. Wu, and C. D. Chen, "Two-dimensional arrays of self-assembled gold and sulfur-containing fullerene nanoparticles," *Langmuir*, vol. 18, pp. 3332–3335, 2002.
- [22] *International Technology Roadmap for Semiconductors*, 1999.